AIP | Review of Scientific Instruments

Lock-in detection for pulsed electrically detected magnetic resonance

Felix Hoehne, Lukas Dreher, Jan Behrends, Matthias Fehr, Hans Huebl, Klaus Lips, Alexander Schnegg, Max Suckert, Martin Stutzmann, and Martin S. Brandt

Citation: Review of Scientific Instruments **83**, 043907 (2012); doi: 10.1063/1.4704837

View online: http://dx.doi.org/10.1063/1.4704837

View Table of Contents: http://scitation.aip.org/content/aip/journal/rsi/83/4?ver=pdfcov

Published by the AIP Publishing

Lock-in detection for pulsed electrically detected magnetic resonance

Felix Hoehne,[1,a)] Lukas Dreher,[1] Jan Behrends,[2,b)] Matthias Fehr,[2,c)] Hans Huebl,[3] Klaus Lips,[2] Alexander Schnegg,[2] Max Suckert,[1] Martin Stutzmann,[1] and Martin S. Brandt[1]

[1]*Walter Schottky Institut, Technische Universität München, Am Coulombwall 4, 85748 Garching, Germany*
[2]*Helmholtz-Zentrum Berlin für Materialien und Energie, Institut für Silizium-Photovoltaik, Kekuléstr. 5, 12489 Berlin, Germany*
[3]*Walther-Meißner-Institut, Bayerische Akademie der Wissenschaften, Walther-Meißner-Str. 8, 85748 Garching, Germany*

(Received 23 November 2011; accepted 2 April 2012; published online 20 April 2012)

We show that in pulsed electrically detected magnetic resonance (pEDMR) signal modulation in combination with a lock-in detection scheme can reduce the low-frequency noise level by one order of magnitude and in addition removes the microwave-induced non-resonant background. This is exemplarily demonstrated for spin-echo measurements in phosphorus-doped silicon. The modulation of the signal is achieved by cycling the phase of the projection pulse used in pEDMR for the readout of the spin state. © *2012 American Institute of Physics*. [http://dx.doi.org/10.1063/1.4704837]

INTRODUCTION

Electron paramagnetic resonance (EPR) has proven to be a powerful tool in the characterization of defects in semiconductors.[1] However, EPR is rather insensitive and typically limited to samples with more than 10^{10} spins.[2] Due to its higher sensitivity, electrically detected magnetic resonance (EDMR) is now widely used to study defects, in particular in indirect, disordered, or organic semiconductors.[3–8] Over the last years, pulsed EDMR (pEDMR) has gained considerable interest, since it combines the large toolbox of pulsed EPR methods[9] with the enhanced sensitivity of EDMR, e.g., to identify spin-dependent transport and recombination processes and study hyperfine interactions.[10–18] However, in many cases, pEDMR suffers from strong low-frequency noise and large non-resonant background signals induced by the strong microwave pulses used to manipulate the spin system.[11] Here, we demonstrate that for pEDMR, a lock-in detection scheme based on a two-step phase cycle[19] is able to subtract the non-resonant background and effectively reduce low-frequency noise by more than one order of magnitude following similar ideas that have been applied in conventional pulsed EPR spectroscopy.[20]

In the pulsed EDMR experiments discussed here, the symmetry of a spin pair is changed by resonant microwave pulses resulting in a change of the recombination rate of excess carriers, which is reflected in a current transient after the microwave pulses. The pEDMR signal is obtained by boxcar integrating the current transient after the pulse sequence over a time interval Δt, resulting in a charge ΔQ proportional to the recombination rate at the end of the pulse sequence,[10] as schematically shown in Fig. 1(a). However, the strong microwave pulses also cause spin-independent non-resonant changes of the current due to, e.g., rectification in the semiconductor sample resulting in additional noise and background signals, which are typically much larger than the spin-dependent signals. These effects can be mitigated by using a lock-in detection scheme for pEDMR measurements, as will be described in the following.

LOCK-IN DETECTION SCHEME

Lock-in detection employs modulation of a signal at a certain frequency and its phase-sensitive detection in combination with bandpass filtering.[21] We will discuss how such a scheme can be implemented in pEDMR exemplarily for the measurement of electrically detected spin echoes. We use a $\pi/2$-τ_1-π-τ_2-$\pi/2$ spin-echo pulse sequence, where $\pi/2$ and π denote microwave pulses with corresponding flipping angles, and τ_1 and τ_2 denote the duration of periods of free evolution [Fig. 1 (a)].[22] Depending on the phase of the projection pulse (indicated in Fig. 1 by $\pm$x), the detection echo-sequence forms an effective 2π pulse for (+x) or an effective π pulse for (−x), since a phase change of 180° results in a reversed sense of rotation of the spin states on the Bloch sphere. Thus, the echo amplitude for a (−x) projection pulse is inverted when compared to a (+x) projection pulse. By repeating the spin-echo pulse sequence N_{cycle} times with a shot repetition time τ_{srt} and inverting the phase for every shot, the signal is square-wave modulated at a frequency $f_{\mathrm{mod}} = 1/(2\tau_{\mathrm{srt}})$. For phase-sensitive detection, the ΔQ detected for (+x) and (−x) are multiplied by +1 and −1, respectively, and the result is averaged over all cycles. As shown below, this scheme is only sensitive to signals within a bandwidth $\Delta f = 1/(2N_{\mathrm{cycle}}\tau_{\mathrm{srt}}) = 1/T_{\mathrm{meas}}$ around the modulation frequency f_{mod}, where T_{meas} denotes the overall measurement time.

In contrast to conventional lock-in detection schemes, the signal in pEDMR is integrated only over the time interval Δt,

a)Author to whom correspondence should be addressed. Electronic mail: hoehne@wsi.tum.de.
b)Present address: Fachbereich Physik, Freie Universität Berlin, Arnimallee 14, 14195 Berlin, Germany.
c)Email: matthias.fehr@helmholtz-berlin.de.

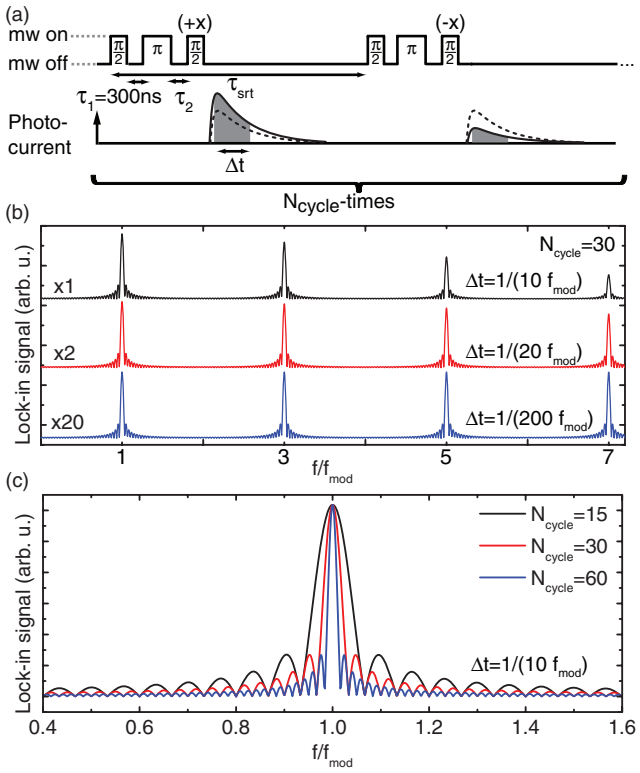

FIG. 1. (a) Pulse sequence to measure electrically detected spin echoes. For signal modulation, we alternately apply the spin-echo pulse sequence with the phase of the last $\pi/2$ pulse set to (+x) and with its phase set to (−x). This cycle is repeated N_{cycle} times. The current transients (solid line) after the mw pulses consist of a spin-independent non-resonant part (dashed line) and a spin-dependent resonant part. After the (−x) spin-echo pulse sequence, the resonant contribution to the current transient is inverted when compared to the current transient after the (+x) pulse sequence. The shaded area indicates the boxcar integration interval Δt. (b) Calculated response of the lock-in detection scheme $\bar{h}(f)$ for different boxcar integration intervals Δt scaled by the indicated factors. (c) Bandwidth calculated for different numbers of cycles N_{cycle}.

which is typically much smaller than the shot repetition time $\tau_{\mathrm{srt}} = 1/(2f_{\mathrm{mod}})$. We therefore calculate the response $h(f)$ of the detection scheme including the boxcar integration interval Δt for an input signal of the form $\sin(2\pi ft + \phi)$ representing a noise component with frequency f and random phase ϕ. The function $h(f, \phi)$ is given by

$$h(f,\phi) = \frac{1}{N_{\mathrm{cycle}}} \sum_{n=0}^{N_{\mathrm{cycle}}-1} \left[\int_{2n\tau_{\mathrm{srt}}}^{2n\tau_{\mathrm{srt}}+\Delta t} \sin(2\pi f t + \phi)\mathrm{d}t - \int_{(2n+1)\tau_{\mathrm{srt}}}^{(2n+1)\tau_{\mathrm{srt}}+\Delta t} \sin(2\pi f t + \phi)\mathrm{d}t \right]. \quad (1)$$

Since the phase of the noise signal is random, the response $h(f, \phi)$ has to be averaged over ϕ, giving

$$\bar{h}(f) = \sqrt{\frac{1}{2\pi}\int_0^{2\pi} h(f,\phi)^2 \mathrm{d}\phi} = \left| \frac{\sin(\pi f \Delta t)\sin(2\pi f N_{\mathrm{cycle}}\tau_{\mathrm{srt}})}{\sqrt{2}\pi f N_{\mathrm{cycle}}\cos(\pi f \tau_{\mathrm{srt}})} \right|. \quad (2)$$

The function $\bar{h}(f)$ is plotted in Fig. 1(b) for different boxcar integration intervals $\Delta t = 1/(10f_{\mathrm{mod}})$, $1/(20f_{\mathrm{mod}})$, and $1/(200f_{\mathrm{mod}})$ with $N_{\mathrm{cycle}} = 30$. The lock-in detection scheme is only sensitive to signals at odd harmonics of f_{mod}. For longer integration intervals Δt, the higher harmonics are suppressed when compared to the fundamental frequency while for short Δt supression is not effective as can be seen for $\Delta t = 1/(200f_{\mathrm{mod}})$ in Fig. 1(b). This can be understood by considering the frequency dependence of the envelope of the peaks, which is determined by the $\sin(\pi f \Delta t)/f$ term of (2). For $f\,\Delta t \ll 1$, this term can be written as $\pi\,\Delta t$, which is independent of the frequency f and therefore all harmonics contribute equally.

In pEDMR, the photocurrent response typically occurs as a transient, which decays within tens of microseconds after the mw pulses,[10] while typical shot repetition times are 1 ms and therefore $f_{\mathrm{mod}}\Delta t = \Delta t/(2\tau_{\mathrm{srt}}) \approx 1/100 \ll 1$. Therefore, the modulated signal contains frequency components at odd multiples of f_{mod} up to a frequency $f \approx 1/\Delta t \approx 50$ kHz. For a cut-off frequency of a high-pass filter $f_{3\mathrm{dB}} = 2$ kHz, typically used to surpress low-frequency current noise, which is larger than the modulation frequency $f_{\mathrm{mod}} < 500$ Hz, the first harmonics are surpressed, but most of the signal at higher harmonics will pass through the filter. The width of the peak at the fundamental frequency (as well as for all harmonics) and therefore the bandwidth of the lock-in detection scheme $\Delta f \propto 1/N_{\mathrm{cycle}}$ and thus $\Delta f \propto 1/T_{\mathrm{meas}}$, as shown in Fig. 1(c) for $\Delta t = 1/(10f_{\mathrm{mod}})$. Repetition of pulse sequences without modulation in combination with signal averaging, as usually employed in pulsed EPR and EDMR, constitutes a low-pass filter centered at 0 Hz with a bandwidth given by the overall measurement time. Modulation of the signal and phase-sensitive detection shifts the center frequency of this filter to the modulation frequency (and its odd harmonics) with the advantage of avoiding low-frequency noise.

MATERIALS AND METHODS

For an experimental demonstration of this detection scheme, we use Si:P epilayers consisting of a 22 nm thick Si layer with a nominal P concentration of 9×10^{16} cm^{-3}, covered with a native oxide and grown on a 2.5 μm thick, nominally undoped Si buffer on a silicon-on-insulator substrate. EDMR signals observed in this type of sample originate dominantly from spin-dependent recombination between ^{31}P donors and Si/SiO$_2$ interface states (P_{b0}).[23] For electrical measurements, interdigit Cr/Au contacts with a spacing of 20 μm covering an active area of 2×2.25 mm^2 are evaporated. All experiments are performed at ~5 K in a dielectric microwave resonator for pulsed EPR at X-band frequencies (Bruker). The samples are illuminated with above-bandgap light and biased with 100 mV resulting in a current of ~60 μA. The current transients after the pulse sequence are amplified by a custom-built balanced transimpedance amplifier (Elektronik-Manufaktur, Mahlsdorf) with low- and high-pass filtering at cut-off frequencies of 1 MHz and 2 kHz, respectively. In all experiments, we choose the microwave frequency and external magnetic field such that the microwave

pulses resonantly excite the spectrally isolated high-field P hyperfine line.[23] The microwave pulses are amplified by a 1 kW traveling-wave tube (Applied Systems Engineering) resulting in a π pulse time of 30 ns. We apply the spin-echo pulse sequence with $N_{cycle} = 1000$ and a shot repetition time $\tau_{srt} = 5$ ms resulting in a modulation frequency of $f_{mod} = 100$ Hz.

RESULTS AND DISCUSSION

In Fig. 2(a), the integrated charge is shown separately for (+x) and (−x) as a function of τ_2 for $\tau_1 = 300$ ns. The echo peaks are visible at $\tau_2 = 300$ ns on top of a large background with positive echo amplitude for (+x) and negative echo amplitude for (−x) while the background is the same for the two phases. To recover the signal, we subtract the two traces from each other resulting in the trace (+x)−(−x), as shown in Fig. 2(b). For comparison, the echo traces (+x) and (−x) after subtraction of the background taken as the smoothed average of the two traces (black line in Fig. 2(a)) are shown as well. In addition to the effective removal of the background, comparison of the noise level in traces (+x) and (−x) with their difference (+x)−(−x) illustrates the considerable reduction of noise by the lock-in detection scheme.

The benefit of this modulation scheme is further demonstrated by measuring the noise as a function of the modulation frequency f_{mod}. To change the modulation frequency f_{mod} independently of the measurement time, in every cycle we repeat the pulse sequence (+x) N_{avr} times followed by

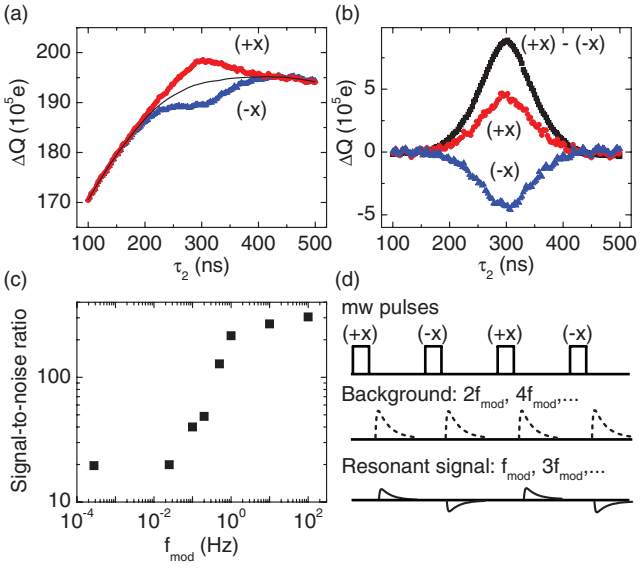

FIG. 2. (a) Integrated charge ΔQ as a function of τ_2 for $\tau_1 = 300$ ns measured with phase modulation at $f_{mod} = 100$ Hz. The data points with the phase of the last $\pi/2$ pulse set to (+x) (upper trace) and (−x) (lower trace) are shown separately. (b) Echo trace obtained by subtracting the two echo traces (+x) and (−x). For comparison, the echo traces (+x) and (−x) after subtraction of the background taken as the smoothed average of the two traces in (a) are shown as well. (c) Signal-to-noise ratio of an electrically detected spin echo as a function of the modulation frequency f_{mod}. (d) Sketch of the non-resonant (dashed lines) and resonant current transients (solid lines) with Fourier components at even multiples and odd mutiples of f_{mod}, respectively.

TABLE I. Summary of the contributions of different parts of the measurement setup to the noise floor at $f_{mod} = 111$ Hz. The different contributions to the noise level are assumed to be independent, so that the squares of their standard deviations can be added to calculate the overall noise level.

	mw pulses only	Current noise only	Current amplifier only	Digital sampling card only	Total setup
σ_{noise} (10^3e)	0.6	0.8	0.4	0.3	1.1

N_{avr} pulse sequences (−x), so that $f_{mod} = 1/(2N_{avr}\tau_{srt})$. Varying N_{avr} and N_{cycle} between 1 and 1000, while keeping the number of sample points $N_{avr} \cdot N_{cycle}$ constant, changes f_{mod} from 0.1 Hz to 100 Hz at a constant bandwidth of $\approx 1/T_{meas} = 0.1$ Hz. The noise is quantified as the standard deviation of 90 measurements of the echo amplitude ΔQ for $\tau_1 = \tau_2 = 300$ ns, where for each measurement, $N_{avr} \cdot N_{cycle} = 1000$ sample points are recorded.

In Fig. 2(c), the signal-to-noise ratio, obtained by dividing the echo peak amplitude by the standard deviation of the noise defined above, is plotted as a function of f_{mod}. By increasing the modulation frequency from several mHz to 100 Hz, the signal-to-noise ratio is improved by more than one order of magnitude. The data point at $f_{mod} = 0.025$ Hz is measured with $\tau_{srt} = 20$ ms, $N_{avr} = 1000$, and $N_{cycle} = 1$, resulting in a four times longer measurement time T_{meas} when compared to the other data points. Since the bandwidth of the lock-in detection scheme $\Delta f \propto 1/T_{meas}$, the obtained noise amplitude is divided by 2 to make it comparable with the other values. The data point at $f_{mod} = 0.3$ mHz is taken without phase modulation. In this case, f_{mod} is calculated as the inverse of the overall measurement time.

To obtain a better understanding of the noise floor at high f_{mod}, we compare the contributions of different parts of the measurement setup to the observed noise level at $f_{mod} = 111$ Hz characterized by the standard deviation σ_{noise} of 90 subsequently taken data points, as described above. The results, as summarized in Table I, show that at high f_{mod}, the noise floor is dominated by the current noise of the illuminated sample with smaller contributions from the microwave pulses and the current measurement setup. However, since the low-frequency components of the current noise of the illuminated sample are effectively filtered out by the 2 kHz high-pass filter of the current amplifier, this noise contribution cannot account for the strong increase of the noise level at low frequencies.

We therefore conclude that the strong decrease of the signal-to-noise ratio at lower frequencies observed in Fig. 2(c) is due to the low-frequency noise of the background current transients induced by the strong microwave pulses. We tentatively attribute this noise to low-frequency variations of the mw pulse amplitude. In X-band pulsed EDMR, the amplitude of the non-resonant current transients induced by the microwave pulses is typically a factor of 5-100 larger than the amplitude of the resonant current transients. Small pulse-to-pulse amplitude variations, which are negligible in pulsed ESR applications, are directly reflected as variations of the amplitude of the current transients and therefore may become the dominant noise source in pulsed EDMR. This noise,

although at low frequencies, is not removed by the high-pass filter, as discussed below.

Since the amplitude of the non-resonant current transients is independent of the phase of the mw pulse, the background signal contains Fourier components at even multiples of f_{mod}, while the Fourier components of the signal occur at odd multiples of f_{mod}, as sketched in Fig. 2(d). Both signals occur on the same timescale and therefore contain Fourier components up to ≈50 kHz, as discussed above. Noise in the amplitude of the mw pulses at frequencies f_{noise} will be mixed with the background signal resulting in noise components at $2f_{mod} \pm f_{noise}$ and higher even harmonics, which are not filtered out by the high-pass filter. However, the lock-in detection scheme is only sensitive to signals at odd harmonics of f_{mod} (see Fig. 1) and, therefore, the low-frequency noise is removed for large f_{mod}, as shown in Fig. 2(c). Since noise at $f_{noise} = f_{mod}$ cannot be removed by lock-in detection, the signal-to-noise ratio decreases for smaller f_{mod} due to the low-frequency noise.

In most pulsed EDMR experiments until now, the large microwave-induced background is removed by measuring additional traces at different values of the static magnetic field, where no resonant processes are observed.[11] In the approach presented here, no additional traces at off-resonance fields have to be measured since the background is subtracted by the lock-in detection scheme. Since for a spin echo without lock-in detection, conventional pEDMR measurements were performed at typically two additional values of the magnetic field, the phase-cycling itself reduces the measurement time by a factor of 3. Together with the tenfold increase of the signal-to-noise ratio due to the lock-in detection, this leads to a reduction of the measurement time by a factor of ∼300. In principle, for pulse sequences, where phase modulation is not feasible, other parameters like the microwave frequency or the magnetic field can be modulated.

CONCLUSIONS

In summary, we have demonstrated theoretically and experimentally a lock-in detection scheme for pulsed EDMR experiments, which significantly improves the signal-to-noise ratio. This scheme allows to extend the experimental methods of pEDMR to more advanced pulse sequences[16,17] and opens its application to other materials and spin-dependent processes to be studied with this technique.

ACKNOWLEDGMENTS

This work was supported by Deutsche Forschungsgemeinschaft (DFG) (Grant No. SFB 631, C3) and BMBF (EPR-Solar, Grant No. 03SF0328).

[1] J.-M. Spaeth and H. Overhof, *Point Defects in Semiconductors and Insulators* (Springer, Berlin, 2003).
[2] D. C. Maier, Bruker Rep. **144**, 13 (1997).
[3] D. J. Lepine, Phys. Rev. B **6**, 436 (1972).
[4] E. L. Frankevich, A. I. Pristupa, and V. M. Kobryanskii, JETP Lett. **40**, 733 (1984).
[5] V. Dyakonov, N. Gauss, G. Rösler, S. Karg, W. Rieß, and M. Schwoerer, Chem. Phys. **189**, 687 (1994).
[6] W. E. Carlos and S. Nakamura, Appl. Phys. Lett. **70**, 2019 (1997).
[7] M. Stutzmann, M. S. Brandt, and M. W. Bayerl, J. Non-Cryst. Solids **266–269**, 1 (2000).
[8] C. F. O. Graeff, G. B. Silva, F. Nüesch, and L. Zuppiroli, Eur. Phys. J. E **18**, 8 (2005).
[9] A. Schweiger and G. Jeschke, *Principles of Pulse Electron Paramagnetic Resonance* (Oxford University Press, Oxford, 2001).
[10] C. Boehme and K. Lips, Phys. Rev. B **68**, 245105 (2003).
[11] A. R. Stegner, C. Boehme, H. Huebl, M. Stutzmann, K. Lips, and M. S. Brandt, Nat. Phy. **2**, 835 (2006).
[12] W. Harneit, C. Boehme, S. Schaefer, K. Huebener, K. Fostiropoulos, and K. Lips, Phys. Rev. Lett. **98**, 216601 (2007).
[13] D. R. McCamey, H. A. Seipel, S.-Y. Paik, M. J. Walter, N. J. Borys, J. M. Lupton, and C. Boehme, Nat. Mat. **7**, 723 (2008).
[14] J. Behrends, A. Schnegg, M. Fehr, A. Lambertz, S. Haas, F. Finger, B. Rech, and K. Lips, Phil. Mag. **89**, 2655 (2009).
[15] J. Behrends, A. Schnegg, K. Lips, E. A. Thomsen, A. K. Pandey, I. D. W. Samuel, and D. J. Keeble, Phys. Rev. Lett. **105**, 176601 (2010).
[16] F. Hoehne, L. Dreher, H. Huebl, M. Stutzmann, and M. S. Brandt, Phys. Rev. Lett. **106**, 187601 (2011).
[17] F. Hoehne, J. Lu, A. R. Stegner, M. Stutzmann, M. S. Brandt, M. Rohrmüller, W. G. Schmidt, and U. Gerstmann, Phys. Rev. Lett. **106**, 196101 (2011).
[18] M. Fehr, J. Behrends, S. Haas, B. Rech, K. Lips, and A. Schnegg, Phys. Rev. B **84**, 193202 (2011).
[19] C. Gemperle, G. Aebli, A. Schweiger, and R. R. Ernst, J. Magn. Res. **82**, 241 (1990).
[20] P. Percival and J. S. Hyde, Rev. Sci. Instrum. **46**, 1522 (1975).
[21] R. H. Dicke, Rev. Sci. Instrum. **17**, 268 (1946).
[22] H. Huebl, F. Hoehne, B. Grolik, A. R. Stegner, M. Stutzmann, and M. S. Brandt, Phys. Rev. Lett. **100**, 177602 (2008).
[23] F. Hoehne, H. Huebl, B. Galler, M. Stutzmann, and M. S. Brandt, Phys. Rev. Lett. **104**, 046402 (2010).